TOWARDS UNDERSTANDING FINE-TUNING MECHANISMS OF LLMS VIA CIRCUIT ANALYSIS

Anonymous authors

ABSTRACT

Fine-tuning significantly improves the performance of Large Language Models (LLMs), yet its underlying mechanisms remain poorly understood. This paper aims to provide an in-depth interpretation of the fine-tuning process through circuit analysis, a popular tool in Mechanistic Interpretability (MI). Unlike previous studies (Prakash et al., 2024; Chhabra et al., 2024) that focus on tasks where pre-trained models already perform well, we develop a set of mathematical tasks where fine-tuning yields substantial performance gains, which are closer to the practical setting. In our experiments, we identify circuits at various checkpoints during fine-tuning and examine the interplay between circuit analysis, fine-tuning methods, and task complexities. First, we find that while circuits maintain high node similarity before and after fine-tuning, their edges undergo significant changes, which is in contrast to the previous work (Prakash et al., 2024; Chhabra et al., 2024) that show circuits only add some additional components after fine-tuning. Based on these observations, we develop a circuit-aware Low-Rank Adaptation (LoRA) method, which assigns ranks to layers based on edge changes in the circuits. Experimental results demonstrate that our circuit-based LoRA algorithm achieves an average performance improvement of 2.46% over standard LoRA with similar parameter sizes. Furthermore, we explore how combining circuits from subtasks can enhance fine-tuning in compositional tasks, providing new insights into the design of such tasks and deepening the understanding of circuit dynamics and fine-tuning mechanisms.

1 INTRODUCTION

Mechanistic Interpretability (MI) has become a powerful approach for exploring the inner workings of machine learning models, particularly Large Language Models (LLMs) Rai et al. (2024). It provides valuable insights into how information flows and transforms across different layers Ferrando et al. (2024). One of the most critical aspects of deploying LLMs in real-world scenarios is fine-tuning Chung et al. (2024). However, the interpretability of how pre-trained models improve during fine-tuning remains limited, and the underlying mechanisms enabling their success across tasks require further investigation.

Many studies in MI regard models as computational graphs Geiger et al. (2021), where circuits are specific subgraphs that perform identifiable functions Wang et al. (2022). Notably, this framework has been successfully applied to various LLMs, revealing emergent behaviors within attention heads and Multi-Layer Perceptrons (MLPs) Heimersheim & Janiak (2023); Burns et al. (2023); Hanna et al. (2023); Gould et al. (2023). Moreover, circuits have recently been leveraged to investigate the fine-tuning process of language models, seeking to understand the mechanisms behind fine-tuning Prakash et al. (2024); Chhabra et al. (2024); Jain et al. (2024). However, these studies often focus on tasks where pre-trained models already perform well (e.g., GPT-2 Radford et al. (2019) achieves around 98% accuracy on the IOI task), or they use general data for fine-tuning rather than domain-specific datasets Prakash et al. (2024). Under such conditions, fine-tuning mainly enhances existing mechanisms (e.g., by adding some attention heads). Consequently, their arguments may not be applicable in more practical fine-tuning scenarios where models initially perform poorly and require fine-tuning on domain data.

To better understand fine-tuning mechanisms in practical settings, it is crucial to focus on tasks where fine-tuning leads to performance improvements. In this work, we design a class of mathematical

tasks on which pre-trained large language models initially perform poorly with low accuracy, yet demonstrates a performance boost after fine-tuned. We employ the *Edge Attribution Patching with Integrated Gradients (EAP-IG)* Hanna et al. (2024) method to identify circuits within both pre-trained and fine-tuned models. Surprisingly, we observe that this approach consistently finds circuits with high faithfulness, even though the two models differ markedly in performance (see §2). To further validate the stability of the discovered circuits, we introduce another circuit metric, *robustness*, which measures the stability of identified circuits by assessing their edge similarity under different perturbation ratios of the dataset. We show that when compared with a randomly initialized transformer model, the pre-trained model, despite exhibiting very low prediction accuracy, can still achieve substantially higher robustness. This finding further supports the validity of the circuits discovered during the fine-tuning process, irrespective of their prediction performance.

Our Main Findings. Based on the circuits analysis techniques and tasks introduced in §2, we provide a comprehensive interpretation of the key factors in the fine-tuning process. Specifically, we focus on three central research questions and summarize our main observations as follows:

1. **(§3) How do circuits evolve during the fine-tuning process?** We use pythia-1.4B-deduped Biderman et al. (2023), gpt-neo-2.7B Black et al. (2021), opt-6.7B Zhang et al. (2022) to fine-tune on five math tasks. By extracting the circuits at each stage of the model during fine-tuning and analyzing these circuits, the circuits identified by EAP-IG demonstrate high fidelity in both pre-trained and fine-tuned models, despite significant performance differences. *We observe that during fine-tuning, circuits gradually converge as modifications to nodes and edges decrease. Meanwhile, new circuits emerge after fine-tuning, with edge changes playing a more significant role in this process.*

2. **(§4) Can circuit insights enhance the fine-tuning process?** We develop a circuit-aware Low-Rank Adaptation (LoRA) method, which assigns higher ranks to layers that have more edge changes in the circuits. We demonstrate across five different mathematical tasks that using circuit insights to optimize the fine-tuning algorithm is effective, significantly improving LoRA's accuracy and parameter efficiency. *Our experiments highlight how Mechanistic Interpretability enhances fine-tuning efficiency, improving performance with fewer parameters using circuit change insights.*

3. **(§5) How capable is the Union Circuit in performing compositional tasks?** To validate our hypothesis, we design a two-step compositional task, such as "(61 - 45) * 45 =". This compositional task was decomposed into an addition/subtraction task and a multiplication/division task and we use the union of the circuits from subtasks to approximate the circuit for the compositional task. *Our results indicate the circuit for the combination task can be approximated by the union of subtask circuits, enhancing the model's performance on the combination task during fine-tuning.*

2   CIRCUIT DISCOVERY AND TASK DESIGN

2.1   CIRCUIT DISCOVERY: EAP-IG

Attribution patching is a technique for identifying circuits using two forward passes and one backward pass Syed et al. (2023). In our experiments, we use Edge Attribution Patching with Integrated Gradients (EAP-IG) Hanna et al. (2024), which addresses computational inefficiency in large models and resolves zero-gradient issues with KL divergence. EAP-IG computes importance scores by integrating gradients along the path between clean and corrupted activations, making it our method of choice. The formula for scoring each edge is:

$$\Delta L(E) \approx \left| (\mathbf{e}_{\text{corr}} - \mathbf{e}_{\text{clean}})^\top \frac{1}{m} \sum_{k=1}^{m} \nabla_{\mathbf{e}_k} L(x) \right|,$$

where $\mathbf{e}_{\text{clean}}$ and $\mathbf{e}_{\text{corr}}$ denote the activations in the circuit under the clean and corrupted inputs. m is the total number of interpolation steps, and k represents the index of a specific step. $\nabla_{\mathbf{e}_k} L(x)$ denotes the gradient of the loss function $L(x)$ with respect to the interpolated activations $\mathbf{e}_k$.

In this study, we choose $m = 5$ based on Hanna et al.'s (2024) recommendations Hanna et al. (2024).

2.2 CIRCUIT EVALUTAION: FAITHFULNESS AND ROBUSTNESS

Faithfulness. Faithfulness serves as a key metric to evaluate the reliability of circuits discovered in MI and it quantifies how closely a circuit replicates the behavior of the original model Wang et al. (2022); Chhabra et al. (2024); Prakash et al. (2024). We adopt Kullback-Leibler divergence (KL-divergence) as the metric, following Conmy et al. Conmy et al. (2023). Let M denote the model and C the discovered circuit. Faithfulness is defined as the percentage of the model's performance captured by the circuit. The formula for faithfulness is:

$$\text{Faithfulness} = \left(1 - \frac{|F(M) - F(C)|}{F(M)}\right) \times 100\%,$$

where $F(M)$ represents the performance of the full model M and $F(C)$ represents the performance of the circuit C.

Robustness. To evaluate the stability of the identified circuit, we propose a robustness score based on its robustness under dataset perturbations. Taking addition and subtraction tasks as an example, perturbations include numeric noise (e.g., changing $7 + 12$ to $7 + 15$), and operator noise (e.g., replacing $12 + 7$ with $12 - 7$). And we conduct robustness calculations on these perturbed datasets, applying noise at varying levels to create noisy datasets.

The robustness score is computed using the Jaccard Similarity Jaccard (1912) between the initial circuit G_0 and perturbed circuits G_p. The formula is:

$$\text{Robustness}(p) = J_E(G_0, G_p),$$

where $J_E(G_0, G_p)$ represents the Jaccard Similarity for **edges** between the initial circuit G_0 and the perturbed circuit G_p, and p denotes the perturbation level.

This modification focuses on edge similarity, as it better reflects structural integrity. A high robustness score indicates that the perturbed circuits maintain a similar edge structure to the original, with a score closer to 1 reflecting a robust circuit structure.

2.3 TASKS DESIGN

To examine the effect of fine-tuning on circuit dynamics, we construct a suite of challenging mathematical tasks in which pre-trained models initially perform poorly. As shown in Figure 1, these tasks help reveal the underlying fine-tuning mechanisms that drive significant performance gains during the process.

Addition and Subtraction (Add/Sub). This task evaluates the model's ability to perform basic addition and subtraction operations. Corrupted data involves altering the arithmetic operation. The task includes five subtasks categorized by the range of numbers involved within 100, 200, 300, 400, and 500. Each subtask contains 5,000 instances.

Multiplication and Division (Mul/Div). This task assesses the model's capability to handle multiplication and division accurately. Corrupted data involves changing the operation between multiplication and division. A total of 2,000 instances are included in this task.

Arithmetic and Geometric Sequence (Sequence). This task measures the model's ability to recognize and extend arithmetic or geometric sequences. Corrupted data involves altering one term in the sequence. The dataset for this task contains 5,000 instances.

Least Common Multiple (LCM). This task tests the model's ability to calculate the Least Common Multiple (LCM) of two integers. Corrupted data involves changing the input numbers or the conditions of the LCM calculation. The task includes 2,500 instances.

Function Evaluation (Function). This task focuses on the model's ability to compute values for linear functions, typically of the form $y = mx + b$. Corrupted data involves altering the constant term in the function. The dataset contains 5,000 instances. For each task, we ensure a strict separation between the dataset used for fine-tuning and the dataset used for circuit analysis. Specifically, 80% of the dataset is allocated for fine-tuning, and the remaining 20% is reserved for identifying circuits and evaluating the model's and circuit's accuracies. This separation guarantees that performance evaluation is conducted on data unseen during fine-tuning.
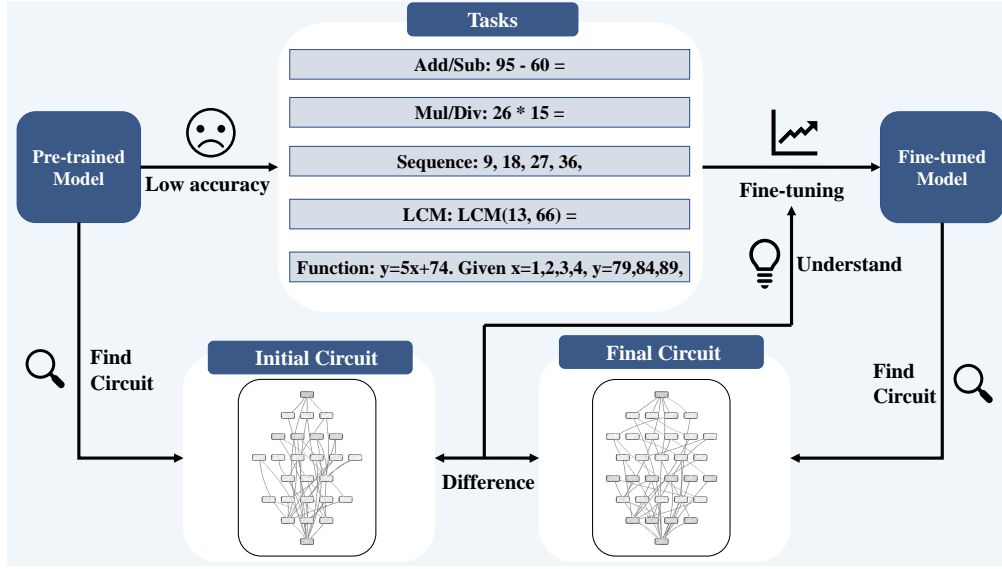
Figure 1: **The workflow of understanding fine-tuning mechanisms using circuits.** The initial pre-trained model shows low accuracy on tasks. The corresponding circuits were found in both the pre-trained model and the fine-tuned model, and the fine-tuning mechanism was understood by comparing the changes in the circuits before and after.

3 How Do Circuits Evolve During the Fine-Tuning Process?

3.1 Model Accuracy, Circuit Faithfulness, and Robustness Analysis

To analyze circuit evolution, we first evaluate model accuracy across fine-tuning checkpoints. We use LoRA Hu et al. (2021) to fine-tune the Pythia-1.4B model Biderman et al. (2023) on five different mathematical tasks. The experimental settings for fine-tuning are shown in Appendix B. The left panel of Figure 2 depicts the accuracy dynamics of the model on five mathematical tasks during fine-tuning. We track the model's accuracy at various training stages across different tasks, revealing consistent improvements in performance throughout the fine-tuning process.

Next, we explore the faithfulness of the circuits found at each stage of fine-tuning. Prior work Hanna et al. (2024) achieved over 85% faithfulness by selecting 1–2% of edges. Given our more complex tasks and larger model, we select 5% of edges to ensure reliable circuits (faithfulness >70%). As shown in the middle panel of Figure 2, circuit faithfulness consistently exceeds 80% across most tasks, both before fine-tuning (Checkpoint 0) and throughout fine-tuning (Checkpoints 1–10). The only exception is Add/Sub task, where faithfulness is 77.52% before fine-tuning. These results confirm high circuit faithfulness in both pre-trained and fine-tuned models across all tasks.

Finally, we conduct robustness analysis on the circuits identified by EAP-IG. We evaluate the robustness of circuits in the pre-trained model, the fine-tuned model, and a randomly initialized model. In this section, we present the robustness analysis for the Add/Sub (100), with analysis for other tasks provided in Appendix D. As discussed in Section 2.2, we perturb the original dataset by 10% to 90% and identify the circuit of three models in perturbed datasets with varying noise levels. Then, we compute the robustness score of Fine-tuned, Pre-trained, and Random models under different perturbation levels. Results in the right part of Figure 2 reveal that circuits identified by EAP-IG demonstrate high fidelity in both pre-trained and fine-tuned models, despite significant performance differences.

> **Key Observation 1:** Circuits can be identified in both pre-trained and fine-tuned models with high faithfulness and robustness, regardless of their significant performance differences.
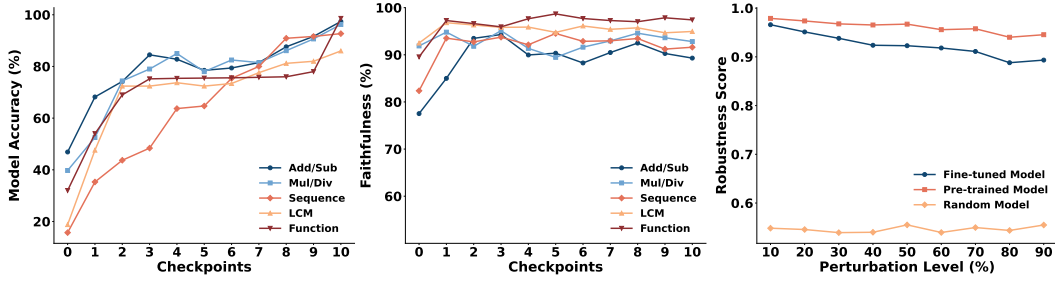
4

Figure 2: **Circuit Accuracy, Faithfulness, and Robustness during Fine-tuning. Left:** Training progress of the model accuracy across different mathematical tasks, showing continuous improvement over checkpoints. **Middle:** Evolution of faithfulness metrics during training, demonstrating consistently high faithfulness across five mathematical tasks. **Right:** Robustness analysis for the Add/Sub task. Robustness evaluation under different perturbation levels, comparing Fine-tuned, Pre-trained, and Random models.

3.2 CIRCUIT IS CONVERGING DURING FINE-TUNING

We conjecture that as the model's accuracy on the task continues to improve, the model's internal circuits should continue to stabilize. To verify our hypothesis, we analyze the change of nodes and edges across consecutive checkpoints.

First, we analyze node and edge changes across checkpoints. The top right of Figure 3 shows three mathematical tasks with increasing model accuracy during fine-tuning. As the model accuracy improves, the number of node and edge changes consistently decreases, indicating circuit stabilization and convergence over time. Additional details for other tasks are provided in Appendix E.

Subsequently, we propose a new metric to measure the degree of change of nodes and edges during fine-tuning. To quantify the changes in edges and nodes during fine-tuning across n checkpoints, we define a unified change rate:

$$\Delta_S = \frac{1}{n} \sum_{t=0}^{n-1} \frac{\Delta s_{t \to t+1}}{S_0} \times 100\%,$$

where $\Delta s_{t \to t+1}$ denotes the number of nodes or edges that change from checkpoint t to checkpoint $t + 1$, and S_0 denotes the total number of nodes or edges in the initial circuit.

As shown in Figure 3, fine-tuning induces structural changes, with Δ_S (Edge) consistently exceeding Δ_S (Node) by a factor of 2–3 across three tasks. This underscores the pivotal role of edges as the primary drivers of structural adaptation during fine-tuning. For the other tasks, the change rates of nodes and edges in the circuit are also shown in Appendix E.

> **Key Observation 2:** Fine-tuning performs more significant edge modifications than node modifications.

3.3 REORGANIZING CIRCUIT EDGES TO FORM A NEW CIRCUIT

As discussed in Section 2.1, each edge's score is computed as the dot product of the averaged loss gradients and activation difference, quantifying its influence on model predictions. To examine structural changes in circuits during fine-tuning, we use the 95th percentile of edge scores as a dynamic threshold. Edges in the initial and final circuits exceeding this threshold are retained, yielding sparser circuits that capture the model's core information flow. Experimental results for all other tasks are provided in Appendix F.

The distribution of added and deleted nodes and edges follows a distinct pattern. As illustrated in the left part of Figure 3, added nodes are predominantly located in the middle and later layers of the circuit, whereas added and deleted edges are concentrated in the middle layers. The shallow layers exhibit minimal changes, providing a stable foundation for task-specific adaptations.
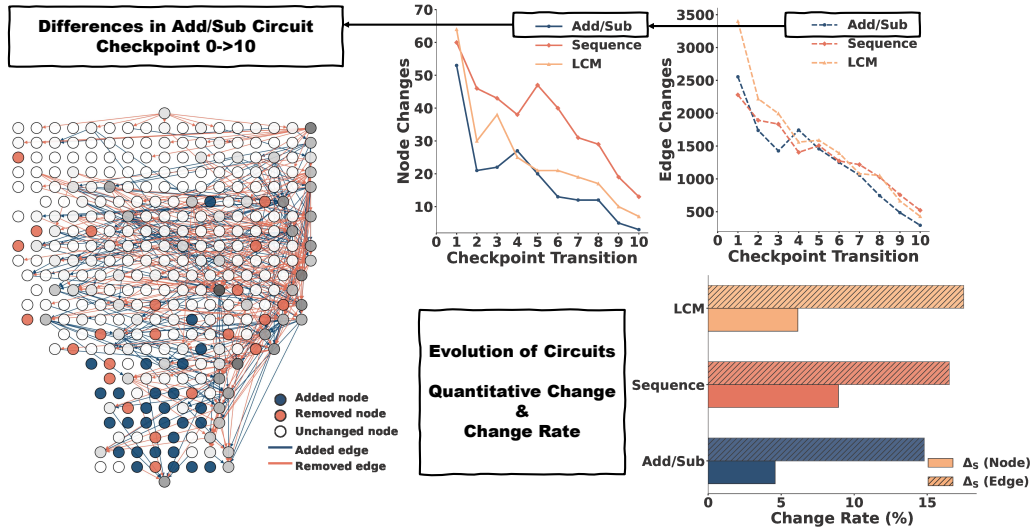
5

Figure 3: **The structural differences of Add/Sub(100) circuit (24 layers) and evolution of circuits across checkpoints in terms of node and edge changes. Left: Differences of Add/Sub(100) circuit before and after fine-tuning.** The layout organizes nodes hierarchically from input to output. Nodes and edges are color-based on their status: added (blue), removed (red), or unchanged (grey/white). Darker grey nodes indicate higher degrees. **Top Right: Node and edge changes between checkpoints during fine-tuning in three tasks.** The left chart depicts the number of node changes per transition, while the right chart focuses on edge changes. **Bottom Right: Change rate of Add/Sub, Sequence, LCM tasks.** Bars with diagonal lines represent the change rate of edges.

In order to prove our conclusions, we conduct investigations into how the circuit evolves under different fine-tuning regimes. Specifically, Appendix G examines the circuit modifications resulting from various PEFT strategies, while Appendix H focuses on the changes induced by full-parameter fine-tuning and LoRA. Finally, Appendix I provides a comparison of circuit changes observed under different LLMs. In these experiments, we also obtain the above key observation.

4 Can Circuit Insights Enhance the Fine-tuning Process?

In the previous section, we observe that while the nodes in the model's circuit exhibit minimal changes during fine-tuning, the edges undergo significant modifications. This observation raises an intriguing question: *Can LoRA be improved by fine-tuning the edges that change the most?* We would like to improve the fine-tuning algorithm from the perspective of **Mechanistic Interpretability**.

4.1 Applying Circuit Edge Changes into LoRA Fine-Tuning

Based on the score of edges and the result of section 2.1, we assume that the most "active" edges play a key role in the fine-tuning process. Also, considering that LoRA is fine-tuned in layers of the model, we want to focus on the layers where the most "active" edges are located.

We propose `CircuitLoRA`, a circuit-aware Low-Rank Adaptation (LoRA) method that incorporates circuit-level analysis to enhance fine-tuning efficiency and performance. `CircuitLoRA` operates in two phases: first, the edges with the largest score changes are analyzed to identify *Critical Layers*; second, higher-rank LoRA modules are assigned to layers with more edge changes, while standard-rank modules are applied to other layers. The complete procedure is detailed in Algorithm 1.

Our hypothesis is that this improved fine-tuning algorithm, which leverages circuit-based analysis, can make better use of the fine-tuning mechanism. In the subsequent section, we investigate this hypothesis, designing experiments across different mathmatical tasks to compare our strategy against full parameter fine-tuning and LoRA baseline.

6

Algorithm 1 `CircuitLoRA`: Improve LoRA Using Circuit-Based Critical Layers Identification

---

Input: Pre-trained model M, Pre-finetuning circuit C_{before}, Post-finetuning circuit C_{after}, LoRA ranks r_o, r_c, Scaling factors α, $\alpha_{critical}$
Phase 1: Critical Layers Identification
Compute edge differences Δ_e between C_{before} and C_{after}
Aggregate Δ_e to layer scores Δ_l and select critical layers $\mathcal{L}_{critical}$
Phase 2: Module Replacement
for each layer $l \in M$ **do**
   if $l \in \mathcal{L}_{critical}$ **then**
      Replace l with `EnhancedLoRALinear` using r_c and $\alpha_{critical}$
   else
      Replace l with `LoRALinear` using r_o and α
   end if
end for
Return: Updated model M^*

Table 1: **Performance metrics (accuracy in percentage) for Add/Sub (300) and four other math tasks across different configurations.** The control groups of `CircuitLoRA` ($r_o = 8, r_c = 32$) are LoRA ($r_o = 16$) and RandomLoRA ($r_o = 8, r_c = 32$), and the control groups of `CircuitLoRA` ($r_o = 32, r_c = 64$) are LoRA ($r_o = 32$) and RandomLoRA ($r_o = 32, r_c = 64$). Here, r_c is the rank for *critical layer* modules, and r_o is the rank for *non-critical layer* modules.

Method	Parameter Ratio	Add/Sub(300)	Mul/Div	Sequence	LCM	Function
Pre-trained	0%	18.30	39.75	15.70	18.80	32.00
Full FT	100%	79.20	95.75	91.50	91.40	100.00
LoRA ($r_o = 2$)	0.1111%	72.60	90.00	67.10	86.40	84.10
LoRA ($r_o = 8$)	0.4428%	78.30	94.25	79.60	91.20	96.80
LoRA ($r_o = 16$)	0.8816%	78.40	95.50	83.40	91.20	97.30
LoRA ($r_o = 32$)	1.7479%	80.50	96.25	92.70	92.80	98.60
CircuitLoRA ($r_o = 8, r_c = 32$)	0.7175%	**82.70**	**96.00**	**92.20**	**92.60**	**99.40**
RandomLoRA ($r_o = 8, r_c = 32$)	0.7175%	77.50	95.50	81.70	90.40	97.70
CircuitLoRA ($r_o = 32, r_c = 64$)	1.4248%	**83.10**	**97.00**	**94.60**	**93.00**	**99.50**
RandomLoRA ($r_o = 32, r_c = 64$)	1.4248%	79.10	95.75	92.10	92.00	98.50

4.2 IMPROVING FINE-TUNING EFFICIENCY AND ACCURACY BY CIRCUIT INSIGHTS

To verify our hypothesis, we perform experiments on a range of arithmetic and mathematical reasoning tasks. The experimental results of **CircuitLoRA** are summarized in two tables. In our experiments, 5 *Critical Layers* are selected. We compare **CircuitLoRA** against control groups including LoRA and RandomLoRA (5 *Critical Layers* are randomly selected). For each method in the experiment, we report the final accuracy as the mean of five runs with different random seeds.

As shown in Table 1, **CircuitLoRA** consistently outperforms baseline methods, including LoRA and RandomLoRA, across all five tasks. For instance, in the "within 300" task, **CircuitLoRA** ($r_o = 8, r_c = 32$) achieves an accuracy of **82.70%**, with fewer training parameters, surpassing RadomLoRA and LoRA. When configured as **CircuitLoRA** ($r_o = 32, r_c = 64$) reaches **83.10%**, outperforming RandomLoRA and LoRA. **CircuitLoRA** experiments on other tasks refer to the Appendix J.

By focusing on the edges with the highest score during fine-tuning, **CircuitLoRA** demonstrates significant improvements in both accuracy and parameter efficiency across various mathematical tasks. The experimental results presented in this study provide a compelling answer to the question posed in Section 4. This approach leverages insights from **Mechanistic Interpretability**, identifying and prioritizing *Critical Layers* where critical changes occur.

> **Key Observation 3:** Circuits can in turn improve fine-tuning with higher accuracy and parameter efficiency across various mathematical tasks.

Table 2: **Overlap for Different Values of** k **in Circuit Comparisons.** The table presents Overlap_k between the Union Circuit and the Combination Circuit. Additionally, circuits from the Add/Sub task are compared with those from the Mul/Div and Sequence tasks as control groups.

Circuit Comparison	$\text{Overlap}_k(\mathcal{C}_1, \mathcal{C}_2)$		
	$k = 100$	$k = 500$	$k = 1000$
Union vs Compositional	69	259	470
Add/Sub vs Mul_Div	51	187	357
Add/Sub vs Sequence	42	156	286

5 How Capable is the Union Circuit in Performing Compositional Tasks?

In this section, we further explore the behavior of circuits in compositional tasks, aiming to investigate whether these tasks can be interpreted through the combination of circuits.

5.1 Compositional Tasks, Compositional Circuits and Union Circuits

In the beginning, we first introduce a series of definitions regarding the composition of tasks and circuits.

Compositional Tasks. A compositional task is composed of multiple interrelated subtasks, each contributing to the overall objective. **Compositional Circuits.** A Compositional Circuit captures the structural and functional dependencies within a compositional task. **Union Circuits.** A Union Circuit is constructed by merging the circuits of all subtasks.

To design the compositional tasks, we consider the two-step operation, which involves the calculation of two different types of mathematical problem, such as addition/subtraction and multiplication/division. For instance, the compositional task '$(61 - 45) \times 45 =$' involves two mathematical operations: (1) (Addition/Subtraction): $61 - 45 =$'; and (2) (Multiplication/Division): $16 \times 45 =$'. More examples of compositional tasks can be found in Appendix K.

Our intuition is that if the circuits can represent the minimum calculation block for one tasks, then it is conjectured that the Union Circuits of the two subtasks can exhibit the power to represent the circuits for the compositional task. In the following, we will investigate the conjecture through two approaches: (1) we compare the similarities between the Union Circuits and the Compositional Circuits; (2) we use the Union Circuits to develop the `CircuitLoRA` algorithm and evaluate whether the performance of the compositional task can also be improved.

5.2 Efficient Single-Phase Fine-Tuning on Compositional Task with Union Circuit

We conduct overlap analysis and fine-tuning experiments on the two-step operation combination task. For a circuit $\mathcal{C}$, we define a $\text{Top}_k(\mathcal{C})$ metric to quantify how many of the top-k edges, ranked by their scores, are shared between two circuits. Then we define the Overlap metric as follows:

$$\text{Overlap}_k(\mathcal{C}_1, \mathcal{C}_2) = \big|\text{Top}_k(\mathcal{C}_1) \cap \text{Top}_k(\mathcal{C}_2)\big|.$$

First, we calculate the Union Circuit and Combination Circuit under the two-step operation combination task.

Through overlap analysis, we prove the efficiency of Union Circuit to a certain extent. Table 2 analyzes the overlap for different values of k to evaluate the efficiency of the Union Circuit. The results show that, regardless of the value of k, the overlap between the Union Circuit and the Compositional Circuit is consistently the highest. Comparisons are made between the addition/subtraction circuit and circuits from control tasks, such as multiplication/division and arithmetic/geometric sequences. The overlaps in these cases are notably lower. These findings demonstrate that the Union Circuit provides an approximate representation of the Compositional Circuit.

8

Table 3: **Performance metrics for Two-Step Operations Task.** `CircuitLoRA`$_C$ represents using Compositional Circuit for *Critical Layer* Identification and `CircuitLoRA`$_U$ represents using Union Circuit. Model Accuracy (M.Acc.) all expressed as percentages.

Method	Parameter Ratio	M.Acc.
Pre-trained	/	0.90
LoRA ($r_o = 2$)	0.1111%	59.60
LoRA ($r_o = 8$)	0.4428%	60.50
LoRA ($r_o = 16$)	0.8816%	61.10
LoRA ($r_o = 32$)	1.7479%	64.70
`CircuitLoRA`$_C$ ($r_o = 8, r_c = 32$)	0.7175%	**67.20**
`CircuitLoRA`$_U$ ($r_o = 8, r_c = 32$)	0.7175%	**65.50**
RandomLoRA ($r_o = 8, r_c = 32$)	0.7175%	62.30

Then, we use Union Circuit and Compositional Circuit to identify the *Critical Layers* to further explore the 'approximation ability" of Union Circuit. Table 3 summarizes the performance of `CircuitLoRA` and LoRA on the two-step operations task. Specifically, `CircuitLoRA` with Compositional Circuit achieves the highest accuracy of **67.20%**. Surprisingly, when using the Union Circuit for *Critical Layer* identification, `CircuitLoRA` achieves **65.50%**, still exceeding the performance of LoRA except the Compositional Circuit configuration.

This demonstrates we can use Union Circuit for single-phase fine-tune. This means that for fine-tuning of the combination task, if we want to use `CircuitLoRA`, we do not need to find its combinational circuit first, but can replace it with the union of the circuits of the subtasks that have been discovered to some extent.

> **Key Observation 4:** The composition of the circuits can effectively represent the circuits of the compositional task.

6 CONCLUSION AND FUTURE WORK

In this paper, we build on circuit analysis to deepen our understanding of fine-tuning and better leverage learned mechanisms. Our findings show that fine-tuning primarily modifying edges rather than merely introducing new components to form new circuits. Building on this insight, we develop a circuit-aware LoRA method. Across multiple tasks, our results demonstrate that incorporating this MI perspective enhances fine-tuning efficiency. Additionally, we show that the composition of subtask circuits effectively represents the circuit of compositional task.

Moving forward, we will explore the following directions. Although our work focused on math tasks, applying circuit-based methods to more tasks would further validate the generality of our insights. Additionally, while our compositional experiments only explore two-step arithmetic, extending this analysis to multi-step or more compositional tasks could provide deeper insights into circuit interactions, enhancing interpretability and fine-tuning efficiency.

IMPACT STATEMENT

Our work provides concrete insights for advancing Mechanistic Interpretability. This deeper understanding of the internal processes guiding model updates paves the way for more efficient, accurate, and trustworthy AI systems. We hope these findings inspire new methods and applications that take advantage of circuit-based analysis to unlock greater transparency, reliability, and performance in LLMs development, and to make better use of the learned mechanisms in these models.

This paper presents work whose goal is to advance the field of Machine Learning. There are many potential societal consequences of our work, none which we feel must be specifically highlighted here.

REFERENCES

Adithya Bhaskar, Alexander Wettig, Dan Friedman, and Danqi Chen. Finding transformer circuits with edge pruning. In *Proceedings of the 38th Conference on Neural Information Processing Systems (NeurIPS), Spotlight*, 2024. URL `https://arxiv.org/abs/2406.16778`. NeurIPS 2024 Spotlight.

Sunit Bhattacharya and Ondřej Bojar. Understanding the role of ffns in driving multilingual behaviour in llms, 2024. URL `https://arxiv.org/abs/2404.13855`.

Stella Biderman, Hailey Schoelkopf, Quentin Gregory Anthony, Herbie Bradley, Kyle O'Brien, Eric Hallahan, Mohammad Aflah Khan, Shivanshu Purohit, USVSN Sai Prashanth, Edward Raff, et al. Pythia: A suite for analyzing large language models across training and scaling. In *International Conference on Machine Learning*, pp. 2397–2430. PMLR, 2023.

Sid Black, Leo Gao, Phil Wang, Connor Leahy, and Stella Biderman. Gpt-neo: Large scale autoregressive language modeling with mesh-tensorflow. *If you use this software, please cite it using these metadata*, 58(2), 2021.

Collin Burns, Haotian Ye, Dan Klein, and Jacob Steinhardt. Discovering latent knowledge in language models without supervision. In *Proceedings of the International Conference on Learning Representations (ICLR)*, 2023. URL `https://arxiv.org/abs/2212.03827`. ICLR 2023.

Vivien Cabannes, Charles Arnal, Wassim Bouaziz, Alice Yang, Francois Charton, and Julia Kempe. Iteration head: A mechanistic study of chain-of-thought, 2024. URL `https://arxiv.org/abs/2406.02128`.

Xingwu Chen and Difan Zou. What can transformer learn with varying depth? case studies on sequence learning tasks. In *Forty-first International Conference on Machine Learning*, 2024.

Xingwu Chen, Lei Zhao, and Difan Zou. How transformers utilize multi-head attention in in-context learning? a case study on sparse linear regression. In *The Thirty-eighth Annual Conference on Neural Information Processing Systems*, 2024.

Vishnu Kabir Chhabra, Ding Zhu, and Mohammad Mahdi Khalili. Neuroplasticity and corruption in model mechanisms: A case study of indirect object identification. In *Proceedings of the ICML 2024 Workshop on Mechanistic Interpretability*, 2024. ICML 2024 Workshop on Mechanistic Interpretability.

Hyung Won Chung, Le Hou, Shayne Longpre, Barret Zoph, Yi Tay, William Fedus, Yunxuan Li, Xuezhi Wang, Mostafa Dehghani, Siddhartha Brahma, et al. Scaling instruction-finetuned language models. *Journal of Machine Learning Research*, 25(70):1–53, 2024.

Roi Cohen, Eden Biran, Ori Yoran, Amir Globerson, and Mor Geva. Evaluating the ripple effects of knowledge editing in language models. *Transactions of the Association for Computational Linguistics*, 12:283–298, 2024.

Arthur Conmy, Augustine Mavor-Parker, Aengus Lynch, Stefan Heimersheim, and Adrià Garriga-Alonso. Towards automated circuit discovery for mechanistic interpretability. In A. Oh, T. Naumann, A. Globerson, K. Saenko, M. Hardt, and S. Levine (eds.), *Advances in Neural Information Processing Systems*, volume 36, pp. 16318–16352. Curran Associates, Inc., 2023.

Ning Ding, Yujia Qin, Guang Yang, Fuchao Wei, Zonghan Yang, Yusheng Su, Shengding Hu, Yulin Chen, Chi-Min Chan, Weize Chen, et al. Parameter-efficient fine-tuning of large-scale pre-trained language models. *Nature Machine Intelligence*, 5(3):220–235, 2023.

Javier Ferrando, Gabriele Sarti, Arianna Bisazza, and Marta R. Costa-jussà. A primer on the inner workings of transformer-based language models, 2024. URL `https://arxiv.org/abs/2405.00208`.

Dan Friedman, Andrew Lampinen, Lucas Dixon, Danqi Chen, and Asma Ghandeharioun. Interpretability illusions in the generalization of simplified models. In *Proceedings of the 41st International Conference on Machine Learning (ICML)*, 2024. URL `https://arxiv.org/abs/2312.03656`. ICML 2024.

Atticus Geiger, Hanson Lu, Thomas Icard, and Christopher Potts. Causal abstractions of neural networks. In M. Ranzato, A. Beygelzimer, Y. Dauphin, P.S. Liang, and J. Wortman Vaughan (eds.), *Advances in Neural Information Processing Systems*, volume 34, pp. 9574–9586. Curran Associates, Inc., 2021. URL `https://proceedings.neurips.cc/paper_files/paper/2021/file/4f5c422f4d49a5a807eda27434231040-Paper.pdf`.

Mor Geva, Roei Schuster, Jonathan Berant, and Omer Levy. Transformer feed-forward layers are key-value memories. In *Proceedings of the 2021 Conference on Empirical Methods in Natural Language Processing (EMNLP)*, 2021. URL `https://arxiv.org/abs/2012.14913`. EMNLP 2021.

Mor Geva, Avi Caciularu, Kevin Ro Wang, and Yoav Goldberg. Transformer feed-forward layers build predictions by promoting concepts in the vocabulary space. In *Proceedings of the 2022 Conference on Empirical Methods in Natural Language Processing (EMNLP)*, 2022. URL `https://arxiv.org/abs/2203.14680`. EMNLP 2022.

Mor Geva, Jasmijn Bastings, Katja Filippova, and Amir Globerson. Dissecting recall of factual associations in auto-regressive language models. In *Proceedings of the 2023 Conference on Empirical Methods in Natural Language Processing (EMNLP)*, 2023. URL `https://arxiv.org/abs/2304.14767`. EMNLP 2023.

Rhys Gould, Euan Ong, George Ogden, and Arthur Conmy. Successor heads: Recurring, interpretable attention heads in the wild, 2023. URL `https://arxiv.org/abs/2312.09230`.

Michael Hanna, Ollie Liu, and Alexandre Variengien. How does gpt-2 compute greater-than?: Interpreting mathematical abilities in a pre-trained language model. In A. Oh, T. Naumann, A. Globerson, K. Saenko, M. Hardt, and S. Levine (eds.), *Advances in Neural Information Processing Systems*, volume 36, pp. 76033–76060. Curran Associates, Inc., 2023.

Michael Hanna, Sandro Pezzelle, and Yonatan Belinkov. Have faith in faithfulness: Going beyond circuit overlap when finding model mechanisms. In *Proceedings of the Conference on Learning Mechanisms (COLM)*, 2024. URL `https://arxiv.org/abs/2403.17806`. COLM 2024.

Peter Hase, Mohit Bansal, Been Kim, and Asma Ghandeharioun. Does localization inform editing? surprising differences in causality-based localization vs. knowledge editing in language models. In A. Oh, T. Naumann, A. Globerson, K. Saenko, M. Hardt, and S. Levine (eds.), *Advances in Neural Information Processing Systems*, volume 36, pp. 17643–17668. Curran Associates, Inc., 2023.

Stefan Heimersheim and Jett Janiak. A circuit for python docstrings in a 4-layer attention-only transformer. *URL: https://www. alignmentforum. org/posts/u6KXXmKFbXfWzoAXn/acircuit-for-python-docstrings-in-a-4-layer-attention-only*, 2023.

Edward J Hu, Yelong Shen, Phillip Wallis, Zeyuan Allen-Zhu, Yuanzhi Li, Shean Wang, Lu Wang, and Weizhu Chen. Lora: Low-rank adaptation of large language models. *arXiv preprint arXiv:2106.09685*, 2021.

Paul Jaccard. The distribution of the flora in the alpine zone. 1. *New phytologist*, 11(2):37–50, 1912.

Samyak Jain, Robert Kirk, Ekdeep Singh Lubana, Robert P. Dick, Hidenori Tanaka, Edward Grefenstette, Tim Rocktäschel, and David Scott Krueger. Mechanistically analyzing the effects of fine-tuning on procedurally defined tasks, 2024. URL `https://arxiv.org/abs/2311.12786`.

Jungyeon Koh, Hyeonsu Lyu, Jonggyu Jang, and Hyun Jong Yang. Faithful and fast influence function via advanced sampling. In *ICML 2024 Workshop on Mechanistic Interpretability*.

Andrew Lee, Xiaoyan Bai, Itamar Pres, Martin Wattenberg, Jonathan K. Kummerfeld, and Rada Mihalcea. A mechanistic understanding of alignment algorithms: A case study on dpo and toxicity, 2024. URL `https://arxiv.org/abs/2401.01967`.

Kenneth Li, Oam Patel, Fernanda Viégas, Hanspeter Pfister, and Martin Wattenberg. Inference-time intervention: Eliciting truthful answers from a language model. In A. Oh, T. Naumann, A. Globerson, K. Saenko, M. Hardt, and S. Levine (eds.), *Advances in Neural Information Processing Systems*, volume 36, pp. 41451–41530. Curran Associates, Inc., 2023.

Vladislav Lialin, Vijeta Deshpande, Xiaowei Yao, and Anna Rumshisky. Scaling down to scale up: A guide to parameter-efficient fine-tuning, 2024. URL `https://arxiv.org/abs/2303.15647`.

Haokun Liu, Derek Tam, Mohammed Muqeeth, Jay Mohta, Tenghao Huang, Mohit Bansal, and Colin A Raffel. Few-shot parameter-efficient fine-tuning is better and cheaper than in-context learning. *Advances in Neural Information Processing Systems*, 35:1950–1965, 2022.

Callum McDougall, Arthur Conmy, Cody Rushing, Thomas McGrath, and Neel Nanda. Copy suppression: Comprehensively understanding an attention head, 2023. URL `https://arxiv.org/abs/2310.04625`.

Kevin Meng, David Bau, Alex Andonian, and Yonatan Belinkov. Locating and editing factual associations in gpt. In S. Koyejo, S. Mohamed, A. Agarwal, D. Belgrave, K. Cho, and A. Oh (eds.), *Advances in Neural Information Processing Systems*, volume 35, pp. 17359–17372. Curran Associates, Inc., 2022.

Kevin Meng, Arnab Sen Sharma, Alex Andonian, Yonatan Belinkov, and David Bau. Mass-editing memory in a transformer, 2023. URL `https://arxiv.org/abs/2210.07229`.

Catherine Olsson, Nelson Elhage, Neel Nanda, Nicholas Joseph, Nova DasSarma, Tom Henighan, Ben Mann, Amanda Askell, Yuntao Bai, Anna Chen, et al. In-context learning and induction heads. *arXiv preprint arXiv:2209.11895*, 2022.

Nikhil Prakash, Tamar Rott Shaham, Tal Haklay, Yonatan Belinkov, and David Bau. Fine-tuning enhances existing mechanisms: A case study on entity tracking. In *Proceedings of the International Conference on Learning Representations (ICLR)*, 2024. URL `https://arxiv.org/abs/2402.14811`. ICLR 2024.

Alec Radford, Jeffrey Wu, Rewon Child, David Luan, Dario Amodei, Ilya Sutskever, et al. Language models are unsupervised multitask learners. *OpenAI blog*, 1(8):9, 2019.

Daking Rai, Yilun Zhou, Shi Feng, Abulhair Saparov, and Ziyu Yao. A practical review of mechanistic interpretability for transformer-based language models, 2024. URL `https://arxiv.org/abs/2407.02646`.

Alessandro Stolfo, Yonatan Belinkov, and Mrinmaya Sachan. A mechanistic interpretation of arithmetic reasoning in language models using causal mediation analysis. In *Proceedings of the 2023 Conference on Empirical Methods in Natural Language Processing (EMNLP)*, 2023. URL `https://arxiv.org/abs/2305.15054`. EMNLP 2023.

Chen Sun, Nolan Andrew Miller, Andrey Zhmoginov, Max Vladymyrov, and Mark Sandler. Learning and unlearning of fabricated knowledge in language models. In *Proceedings of the ICML 2024 Workshop on Mechanistic Interpretability*, 2024. URL `https://arxiv.org/abs/2410.21750`. ICML 2024 Workshop on Mechanistic Interpretability.

Aaquib Syed, Can Rager, and Arthur Conmy. Attribution patching outperforms automated circuit discovery. In *Proceedings of the NeurIPS 2023 ATTRIB Workshop*, 2023. URL `https://arxiv.org/abs/2310.10348`. NeurIPS 2023 ATTRIB Workshop.

Jesse Vig, Sebastian Gehrmann, Yonatan Belinkov, Sharon Qian, Daniel Nevo, Simas Sakenis, Jason Huang, Yaron Singer, and Stuart Shieber. Causal mediation analysis for interpreting neural nlp: The case of gender bias, 2020. URL `https://arxiv.org/abs/2004.12265`.

Kevin Wang, Alexandre Variengien, Arthur Conmy, Buck Shlegeris, and Jacob Steinhardt. Interpretability in the wild: a circuit for indirect object identification in gpt-2 small, 2022. URL `https://arxiv.org/abs/2211.00593`.

Mengru Wang, Yunzhi Yao, Ziwen Xu, Shuofei Qiao, Shumin Deng, Peng Wang, Xiang Chen, Jia-Chen Gu, Yong Jiang, Pengjun Xie, Fei Huang, Huajun Chen, and Ningyu Zhang. Knowledge mechanisms in large language models: A survey and perspective. In *Proceedings of EMNLP 2024 Findings*, pp. 1–39, 2024. URL `https://arxiv.org/abs/2407.15017`. EMNLP 2024 Findings; 39 pages (v4).

Wenhao Wu, Yizhong Wang, Guangxuan Xiao, Hao Peng, and Yao Fu. Retrieval head mechanistically explains long-context factuality, 2024. URL `https://arxiv.org/abs/2404.15574`.

Qingru Zhang, Minshuo Chen, Alexander Bukharin, Nikos Karampatziakis, Pengcheng He, Yu Cheng, Weizhu Chen, and Tuo Zhao. Adalora: Adaptive budget allocation for parameter-efficient fine-tuning. In *Proceedings of the 11th International Conference on Learning Representations (ICLR)*, 2023. URL `https://arxiv.org/abs/2303.10512`. ICLR 2023.

Shaolei Zhang, Tian Yu, and Yang Feng. Truthx: Alleviating hallucinations by editing large language models in truthful space. In *Proceedings of the 62nd Annual Meeting of the Association for Computational Linguistics (ACL)*, 2024. URL `https://arxiv.org/abs/2402.17811`. ACL 2024 Main Conference.

Susan Zhang, Stephen Roller, Naman Goyal, Mikel Artetxe, Moya Chen, Shuohui Chen, Christopher Dewan, Mona Diab, Xian Li, Xi Victoria Lin, Todor Mihaylov, Myle Ott, Sam Shleifer, Kurt Shuster, Daniel Simig, Punit Singh Koura, Anjali Sridhar, Tianlu Wang, and Luke Zettlemoyer. Opt: Open pre-trained transformer language models, 2022. URL `https://arxiv.org/abs/2205.01068`.

Hongyun Zhou, Xiangyu Lu, Wang Xu, Conghui Zhu, Tiejun Zhao, and Muyun Yang. Lora-drop: Efficient lora parameter pruning based on output evaluation, 2024. URL `https://arxiv.org/abs/2402.07721`.

A RELATED WORK

A.1 MECHANISTIC INTERPRETABILITY

Mechanistic Interpretability investigates how components in large language models process and represent information Wang et al. (2024). At present, many MI studies have been applied in various fields of AI Safety. For instance, oversimplified probes risk Friedman et al. (2024), unlearning fabricated knowledge Sun et al. (2024), reducing toxicity via alignment Lee et al. (2024), mitigating hallucinations by editing representations Zhang et al. (2024), and generating truthful outputs through inference-time interventions Li et al. (2023). Other studies explore how local model edits propagate across tasks Cohen et al. (2024); Meng et al. (2023), Multi-Head Attention in-context learning Chen et al. (2024); Chen & Zou (2024) and enhance influence-function sampling Koh et al.. Specifically, our study examines how circuits evolve during fine-tuning for mathematical tasks, focusing on node and edge changes to reveal mechanisms behind performance improvements.

A.2 CIRCUIT ANALYSIS AND FINE-TUNING

One direction of Circuit Analysis focuses on building complete circuits. Early work localizes factual associations in mid-layer modules Meng et al. (2022) and uses causal mediation to uncover biases Vig et al. (2020); Hase et al. (2023). Automated methods like Automated Circuit Discovery identify significant units Conmy et al. (2023), while techniques like attribution patching, and refine circuit extraction by handling near-zero gradients Syed et al. (2023); Hanna et al. (2024). Edge pruning Bhaskar et al. (2024) provide insights into building the edge of the circuit. Another line of research investigates the functional roles of circuit components, such as Attention heads Wu et al. (2024); McDougall et al. (2023); Olsson et al. (2022); Gould et al. (2023); Cabannes et al. (2024) and Feed Forward Networks (FFNs) / MLPs Geva et al. (2021; 2022); Bhattacharya & Bojar (2024). Additionally, circuits have been used to analyze specific tasks, such as factual knowledge retrieval Geva et al. (2023), arithmetic computation Stolfo et al. (2023), Greater Than task Hanna et al. (2023), and circuit recognition in Indirect Object Identification Wang et al. (2022). Unlike these analyses, which focus on smaller-scale tasks and models, our work offers a new lens on how circuits evolve specifically during fine-tuning on mathematical tasks, revealing crucial roles of edge changes.

As pre-trained language models scale, fine-tuning methods have emerged, optimizing only a small subset of parameters Ding et al. (2023). Parameter-efficient fine-tuning (PEFT) methods, such as LoRA Hu et al. (2021), reduce computational costs while preserving functionality Ding et al. (2023). Advances in LoRA, including pruning Zhou et al. (2024) and adaptive budget allocation Zhang et al. (2023); Liu et al. (2022); Lialin et al. (2024), further improve efficiency. In our study, we introduce a circuit-aware LoRA approach that adaptively assigns higher ranks to layers with more edge changes, boosting efficiency and accuracy in mathematical tasks, and further illustrates how combining circuits from subtasks can enhance performance in compositional tasks during fine-tuning.

B EXPERIMENTAL SETUP OF FINE-TUNING

Fine-tuning experiments were conducted across various arithmetic tasks, with configurations tailored to each. All tasks were trained with a batch size of 8, gradient accumulation steps of 4, and a warmup of 50 steps, using a weight decay of 0.01.

Addition and Subtraction (Add/Sub) task, which includes subtasks with ranges of 100, 200, 300, 400, and 500, each subtask consists of 5,000 samples. The 100-range subtask was trained for 2 epochs, while others were trained for 4 epochs. LoRA experiments were performed with ranks $r = 2, 8, 16, 32$, using a learning rate of 3e-4, except for the 400-range ($r = 32$, lr=2e-4). Full Parameter Fine-Tuning (FPFT) used learning rates of 8e-6 (100-range), 6e-6 (200-range), 5e-6 (400-range), and 4e-6 (500-range). `CircuitLoRA` applied higher learning rates (4e-4 or 5e-4) for *Critical Layers* and 3e-4 for *non-Critical Layers*.

Multiplication and Division (Mul/Div) task contains 2,000 samples and was trained for 2 epochs. LoRA used a learning rate of 3e-4, FPFT used 4e-6, and `CircuitLoRA` used 2e-4 for *Critical Layers* and 3e-4 for *non-Critical Layers*.

756
757
758
759
760
761
762
763
764
765
766
767
768
769
770
771
772
773
774
775
776
777
778
779
780
781
782
783
784
785
786
787
788
789
790
791
792
793
794
795
796
797
798
799
800
801
802
803
804
805
806
807
808
809

Arithmetic and Geometric Sequence (Sequence) task includes 5,000 samples, trained for 4 epochs. LoRA experiments used a learning rate of 3e-4, FPFT used 8e-6, and `CircuitLoRA` applied 6e-4 ($r = 32$) and 5e-4 ($r = 64$) for *Critical Layers*, with 3e-4 for *non-Critical Layers*.

Least Common Multiple (LCM) task, which contains 2,500 samples and was trained for 2 epochs, LoRA used learning rates of 3e-4 ($r = 2, 8$), 4e-4 ($r = 16$), and 2e-4 ($r = 32$). FPFT used 4e-6, and `CircuitLoRA` used 4e-4 ($r = 32$) and 6e-5 ($r = 64$) for *Critical Layers*, with 3e-4 for *non-Critical Layers*.

Function Evaluation (Function) task, with 5,000 samples trained for 2 epochs, used consistent LoRA learning rates of 3e-4 ($r = 2, 8, 16, 32$), FPFT with 8e-6, and `CircuitLoRA` with 4e-4 for *Critical Layers* and 3e-4 for *non-Critical Layers*.

C MODEL ACCURACY AND CIRCUIT FAITHFULNESS ON OTHER TASKS
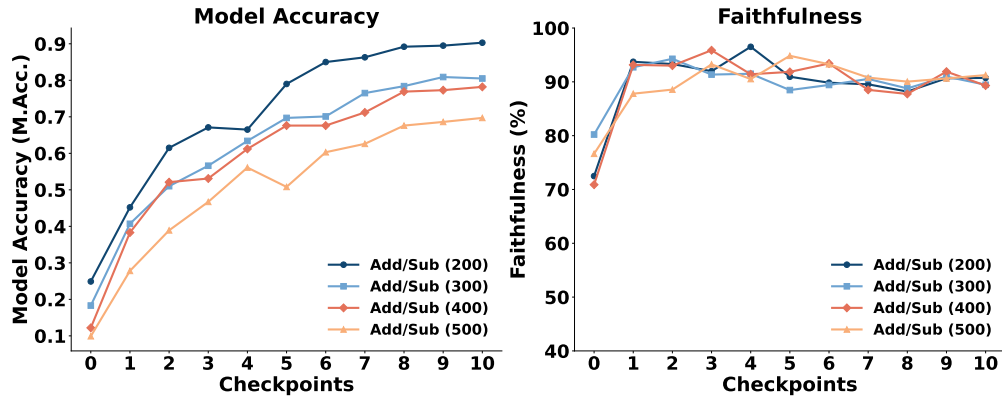

Figure 4: **Performance analysis of Add/Sub tasks across different checkpoints. Left:** Model Accuracy (M.Acc.) shows the performance trends of four tasks—*Add/Sub (200)*, *Add/Sub (300)*, *Add/Sub (400)*, and *Add/Sub (500)* across checkpoints. **Right:** Faithfulness scores measure the reliability of predictions for the same tasks across the same checkpoints.

The left part of Figure 4 presents the model's accuracy for four task and the results indicate a consistent improvement in accuracy across all tasks.

The right part of Figure 4 illustrates the faithfulness of circuits for the same tasks. Faithfulness scores remain above 70% for all tasks. These results highlight both the accuracy improvements and the reliability of circuits throughout the fine-tuning process.

D ROBUSTNESS ANALYSIS EXPERIMENTS ON OTHER TASKS

Building on the results reported in the main text, this appendix details our additional robustness experiments conducted across multiple arithmetic tasks. Following the methodology presented in Section 2.2, we systematically apply input perturbations to Multiplication/Division, Arithmetic/Geometric Sequence, Least Common Multiple, and Function Evaluation tasks. Our findings further corroborate the consistency and fidelity of circuits identified by EAP-IG, demonstrating their ability to adapt under varying perturbation conditions while preserving core computational relationships.

Multiplication and Division Tasks Data perturbation in multiplication and division tasks involves altering one of the operands within a specified range while maintaining the validity of the operation. This introduces variability without disrupting the fundamental arithmetic relationship.

Example:

- `Original:  Calculate the result of the following arithmetic`
  `expression and provide only the final answer:  26 * 15 =`

```
• Perturbed:  Calculate the result of the following arithmetic
  expression and provide only the final answer:  26 * 20 =
```

Arithmetic and Geometric Sequence Tasks   For arithmetic sequences, perturbation is achieved by uniformly shifting each term by a fixed integer. In geometric sequences, the first term is adjusted, and subsequent terms are recalculated using the original common ratio to preserve the sequence's structure.

Example:

```
• Original:  Derive the following sequence:  26, 66, 106, 146,

• Perturbed:  Derive the following sequence:  21, 61, 101,
  141,
```

Least Common Multiple (LCM) Tasks   Data perturbation for LCM tasks involves regenerating the last LCM expression using one of three strategies: generating multiples, coprimes, or pairs with common factors that are not multiples. This ensures diversity and prevents redundancy in the dataset.

Example:

```
• Original:  Calculate the least common multiple (LCM) of two
  numbers.  LCM(189, 84) = 756, LCM(200, 400) =

• Perturbed:  Calculate the least common multiple (LCM) of two
  numbers.  LCM(189, 84) = 756, LCM(75, 120) =
```

Function Evaluation Tasks   In function evaluation tasks, perturbation involves modifying the constant term b in a linear function $y = ax + b$ by a value within a specified range. The corresponding y-values are recalculated to reflect the change, ensuring the functional relationship remains intact.

Example:

```
• Original:  There is a function y=5x+201.  Given x=1,2,3,4,
  y=206,211,216,

• Perturbed:  There is a function y=5x+151.  Given x=1,2,3,4,
  y=156,161,166,
```

In line with the observations for addition and subtraction, our experiments on LCM, Sequence, Multiplication/Division, and Function Evaluation tasks demonstrate that circuits can be identified in both pre-trained and fine-tuned models with high faithfulness and robustness. This finding holds true despite the significant performance gap between the two model states, underscoring the reliability and stability of the discovered circuits across diverse arithmetic tasks.

E   NODE, EDGE, AND CHANGE RATE ANALYSIS ON OTHER TASKS

This section combines the analysis of node and edge changes with the change rates for various tasks. By evaluating these metrics together, we provide a comprehensive view of the structural and dynamic adjustments observed across different tasks. The node and edge changes reflect the structural variations in the underlying data or models, while the change rate quantifies the intensity of these changes, offering deeper insights into task-specific behaviors.

The Figure 6 presents an analysis of node and edge dynamics during fine-tuning across six tasks: Within 200, Within 300, Within 400, Within 500, Multiplication/Division, and Function Evaluation. It highlights how the interplay between node, edge, and change rate metrics contributes to the overall task dynamics, ensuring a holistic understanding of the transformations involved in each scenario.

864
865
866
867
868
869
870
871
872
873
874
875
876
877
878
879
880
881
882
883
884
885
886
887
888
889
890
891
892
893
894
895
896
897
898
899
900
901
902
903
904
905
906
907
908
909
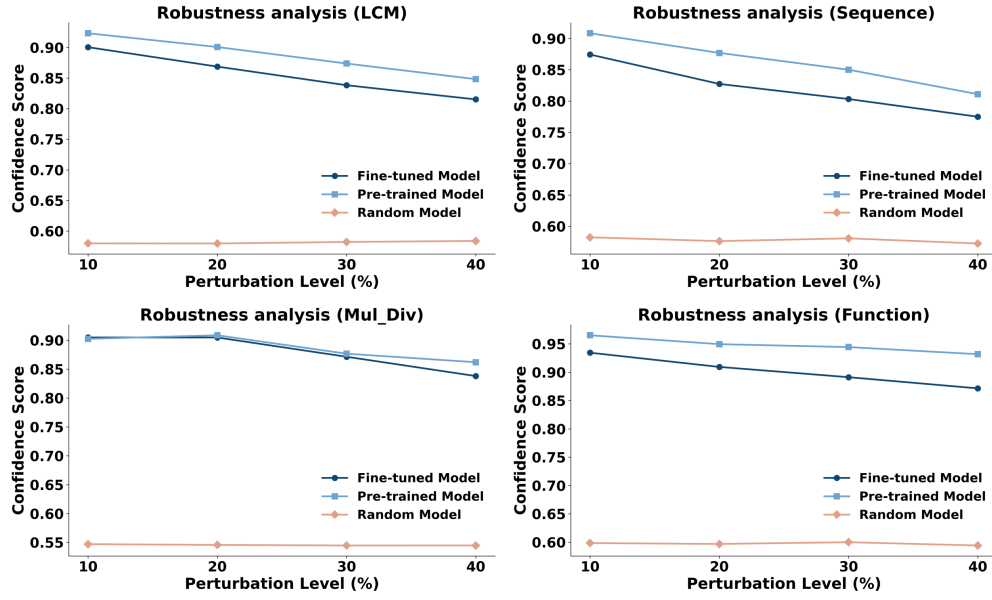910
911
912
913
914
915
916
917

Figure 5: **Robustness analysis across four additional tasks: LCM, Sequence, Mul/Div, and Function.** Despite the varying perturbation levels, both the pre-trained and fine-tuned models exhibit consistently high confidence scores compared to the randomly initialized model.
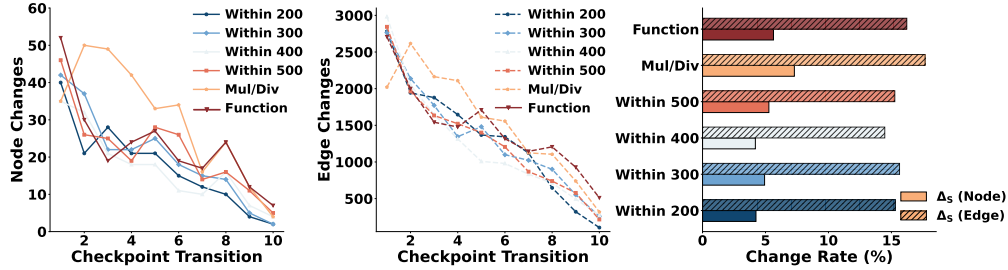

Figure 6: **Analysis of Node and Edge Changes Across Add/Sub Tasks, including Within 200, Within 300, Within 400, Within 500, Multiplication/Division, and Function Evaluation. Left:** Node changes during fine-tuning. **Middle:** Edge changes during fine-tuning. **Right:** Change rates for nodes and edges across tasks.

F CHANGES IN CIRCUITS BEFORE AND AFTER FINE-TUNING IN OTHER TASKS

In this section, we compare the circuits before and after fine-tuning for tasks involving addition and subtraction within the ranges of 200, 300, 400, and 500, as well as tasks on Multiplication and Division, Arithmetic and Geometric Sequence, Least Common Multiple, and Function Evaluation. Please refer to Figures 7, 8, 9, and 10 for the comparison results of all tasks before and after fine-tuning.

Common Observations: The distribution of added and deleted nodes and edges follows a distinct pattern. Our analysis reveals similarities with the findings from addition and subtraction tasks within the range of 100. Same as Figure 3 in Section 3.3, added nodes predominantly appear in the middle and later layers of the circuit. Similarly, added and deleted edges are concentrated in the middle layers. In contrast, the shallow layers exhibit minimal changes, serving as a stable foundation for task-specific adaptations.

918
919
920
921
922
923
924
925
926
927
928
929
930
931
932
933
934
935
936
937
938
939
940
941
942
943
944
945
946
947
948
949
950
951
952
953
954
955
956
957
958
959
960
961
962
963
964
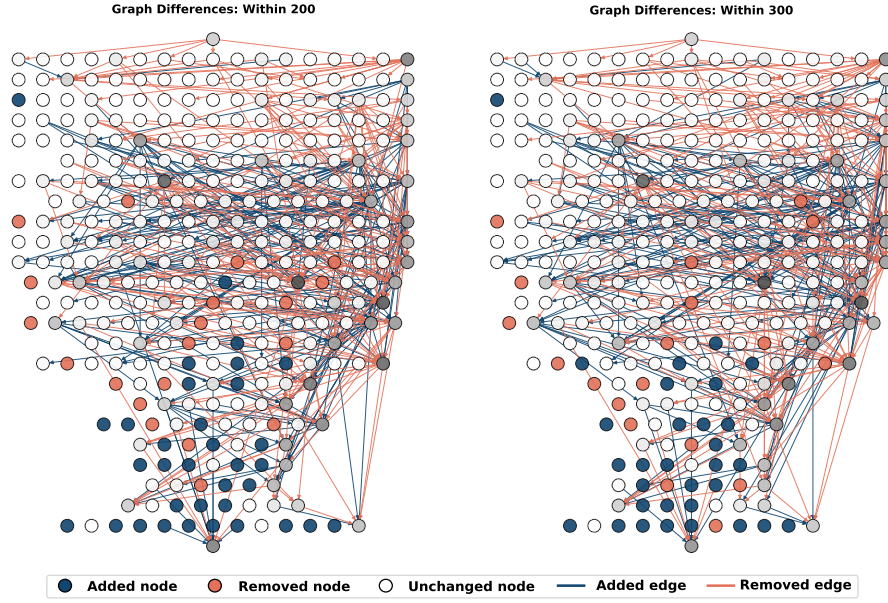965
966
967
968
969
970
971

Figure 7: **Differences of Add/Sub(200) and Add/Sub(300) circuit (24 layers).** Darker gray indicates a higher node degree.

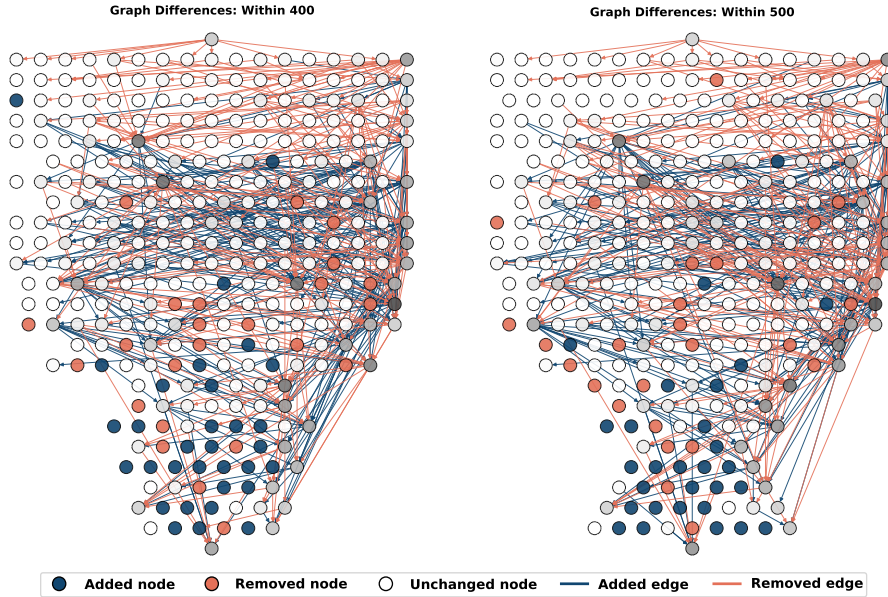Figure 8: **Differences of Add/Sub(400) and Add/Sub(500) circuit (24 layers).** Darker gray indicates a higher node degree.

Trends with Increasing Number Ranges in Addition and Subtraction: We observe a distinct trend in the circuits fine-tuned for addition and subtraction tasks as the number range increases. The edges in the fine-tuned circuits become more concentrated, reflecting a refined structure to handle the broader numeric range efficiently.

Comparative Observations Across Tasks: Tasks such as Multiplication and Division, Arithmetic and Geometric Sequence, Least Common Multiple, and Function Evaluation exhibit different circuit
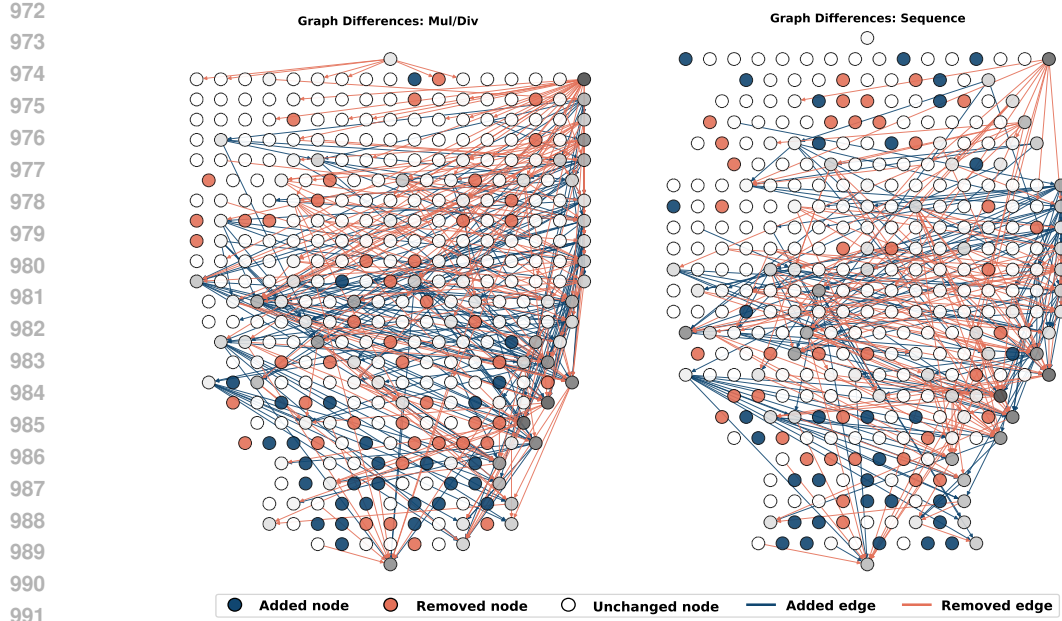
18

Figure 9: **Differences of Mul/Div and Sequence circuit (24 layers).** Darker gray indicates a higher node degree.
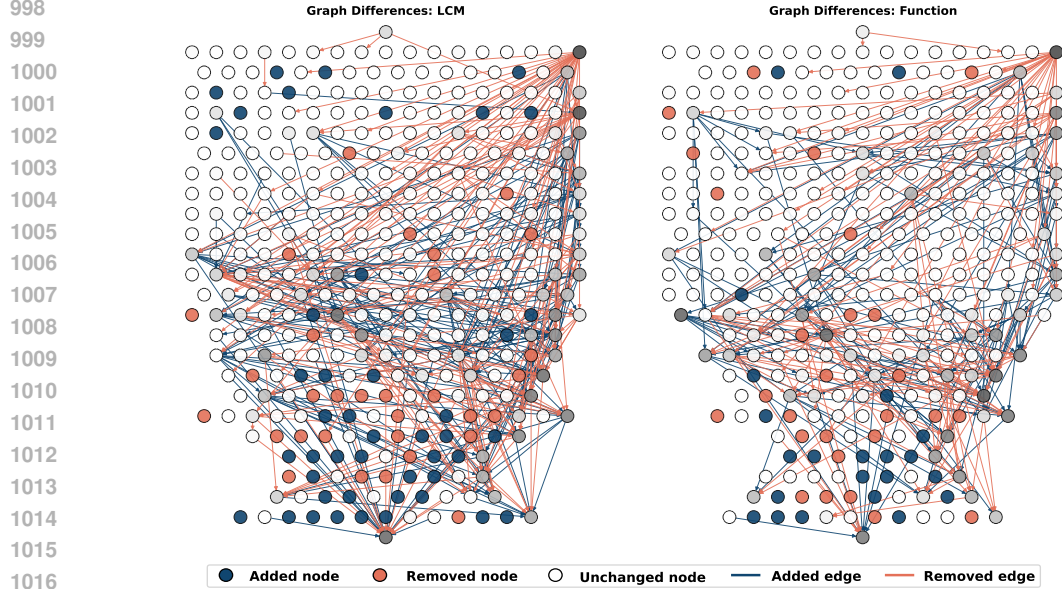

Figure 10: **Differences of LCM and Function circuit (24 layers).** Darker gray indicates a higher node degree.

adaptations compared to addition and subtraction tasks. As illustrated in Figures 9 and 10, these tasks utilize circuits that focus more on the later layers. This difference indicates a shift in computational emphasis, highlighting the tailored adaptations of the circuit for distinct task requirements.

G CIRCUIT CHANGES DURING FINE-TUNING: A COMPARISON ACROSS PEFT METHODS

In this appendix, we compare three different PEFT methods—*LoRA*, *AdaLoRA*, and *IA3* across various mathematical tasks (e.g., addition/subtraction with 200, multiplication/division, Sequence, LCM, and Function). Figures 11 through 15 illustrate the model accuracy, faithfulness, and the evolution of nodes and edges at each checkpoint, as well as the corresponding change rates. By examining these metrics, we can observe how the internal circuits of each model evolve during fine-tuning until they converge.
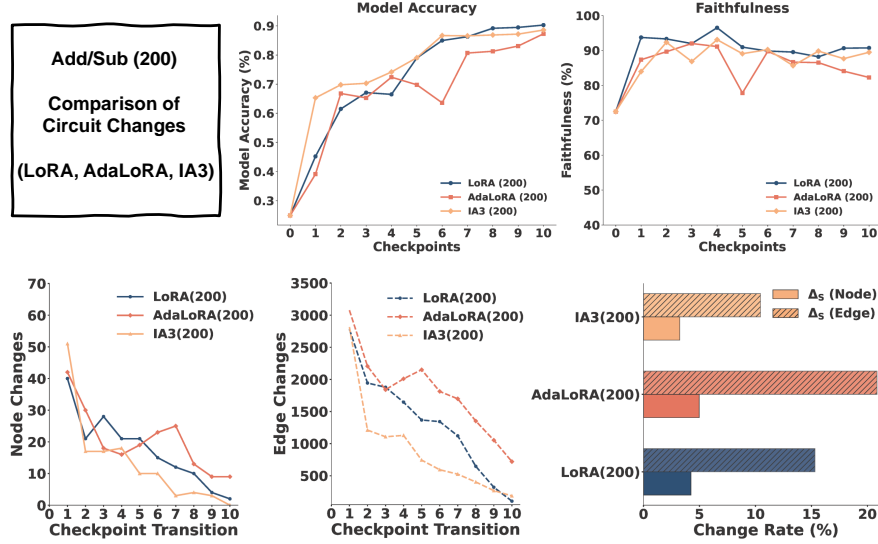

Figure 11: **Comparison of Add/Sub (200) circuits during fine-tuning with LoRA, AdaLoRA, and IA3. Top:** Model accuracy and faithfulness across checkpoints. **Bottom Left:** Node and edge changes across checkpoint transitions. **Bottom Right:** Change rate of nodes and edges during fine-tuning.

The three PEFT methods each create new circuits after fine-tuning on different mathematical tasks. Additionally, we draw the following conclusions:

1. **Across different PEFT methods (LoRA, AdaLoRA, IA3) and diverse math tasks, as model accuracy improves, the circuits converge while edges undergo more significant modifications than nodes, consistent with previous observations.**

2. **Moreover, IA3 has lower node and edge change rates compared to the other two PEFT methods, which can be attributed to its smaller number of trainable parameters.**

Hence, the choice among these three PEFT methods does not alter our primary conclusions that edges exhibit greater changes than nodes, and that the circuits ultimately converge as accuracy increases.

H CIRCUIT CHANGES DURING FINE-TUNING: FULL PARAMETER FINE-TUNING VS. LORA

This appendix compares the circuit changes during fine-tuning between Full Parameter Fine-Tuning (Full-FT) and LoRA. Figure 16 presents the model accuracy and faithfulness at different checkpoints, along with the node and edge modifications and their respective change rates. By examining these metrics, we can observe the similarities and differences in circuit evolution under these two fine-tuning approaches.

Full parameter fine-tuning and LoRA exhibit highly similar convergence trends in circuit evolution. Therefore, both full parameter fine-tuning and parameter-efficient fine-tuning can create

1080
1081
1082
1083
1084
1085
1086
1087
1088
1089
1090
1091
1092
1093
1094
1095
1096
1097
1098
1099
1100
1101
1102
1103
1104
1105
1106
1107
1108
1109
1110
1111
1112
1113
1114
1115
1116
1117
1118
1119
1120
1121
1122
1123
1124
1125
1126
1127
1128
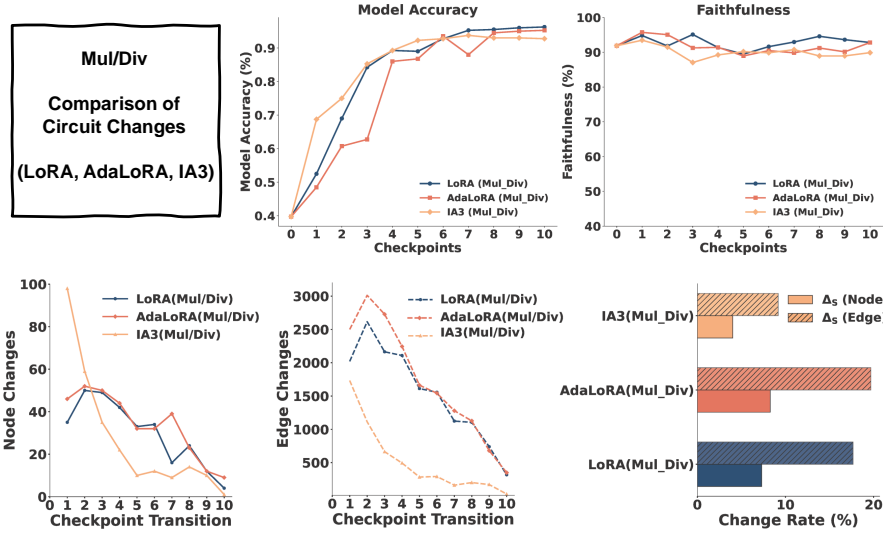1129
1130
1131
1132
1133

Figure 12: **Comparison of Mul/Div circuits during fine-tuning with LoRA, AdaLoRA, and IA3.** **Top:** Model accuracy and faithfulness across checkpoints. **Bottom Left:** Node and edge changes across checkpoint transitions. **Bottom Right:** Change rate of nodes and edges during fine-tuning.
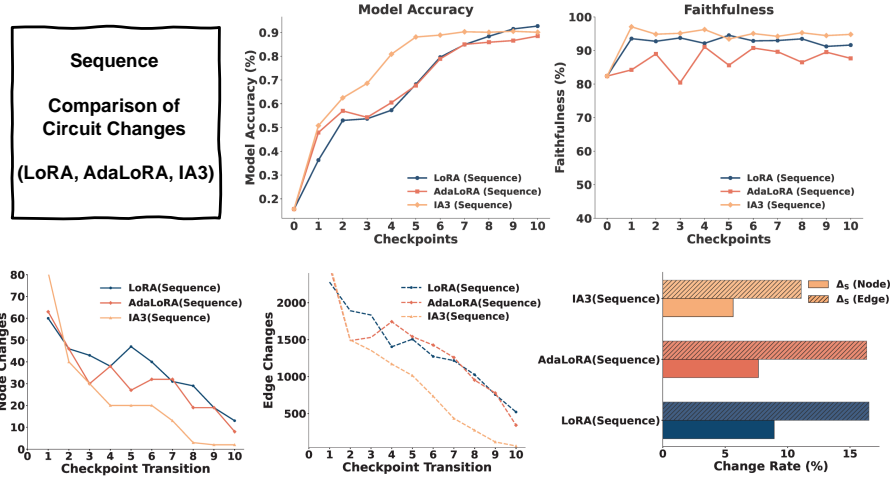

Figure 13: **Comparison of Sequence circuits during fine-tuning with LoRA, AdaLoRA, and IA3.** **Top:** Model accuracy and faithfulness across checkpoints. **Bottom Left:** Node and edge changes across checkpoint transitions. **Bottom Right:** Change rate of nodes and edges during fine-tuning.

new circuit structures. In full parameter fine-tuning, the changes in edges are significantly greater than those in nodes, which is consistent with the previous findings using LoRA.

I CIRCUIT CHANGES DURING FINE-TUNING: A COMPARISON ACROSS DIFFERENT LARGE LANGUAGE MODELS

In this appendix, we compare circuit changes across different large language models (LLMs), including *pythia-1.4B-deduped*, *gpt-neo-2.7B*, and *opt-6.7B*. Figure 17 illustrates their accuracy and faithfulness during fine-tuning, as well as the modifications of nodes and edges through the

21

1134
1135
1136
1137
1138
1139
1140
1141
1142
1143
1144
1145
1146
1147
1148
1149
1150
1151
1152
1153
1154
1155
1156
1157
1158
1159
1160
1161
1162
1163
1164
1165
1166
1167
1168
1169
1170
1171
1172
1173
1174
1175
1176
1177
1178
1179
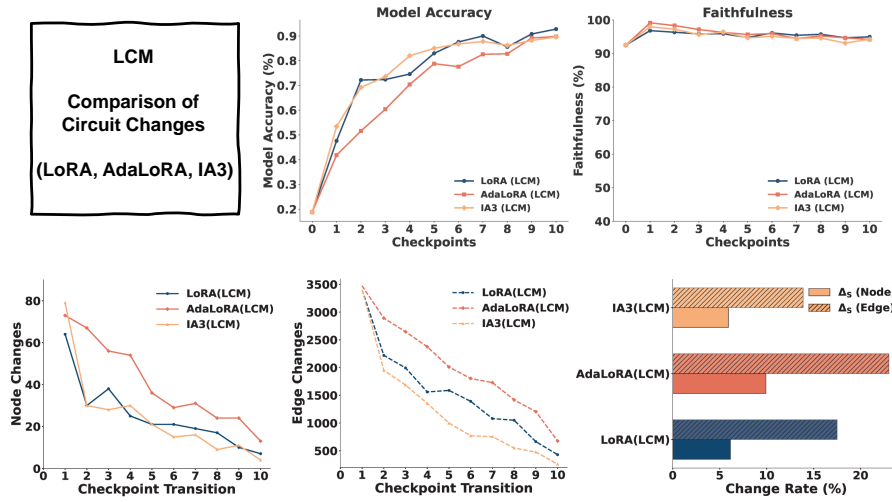1180
1181
1182
1183
1184
1185
1186
1187

Figure 14: **Comparison of LCM circuits during fine-tuning with LoRA, AdaLoRA, and IA3.** **Top:** Model accuracy and faithfulness across checkpoints. **Bottom Left:** Node and edge changes across checkpoint transitions. **Bottom Right:** Change rate of nodes and edges during fine-tuning.
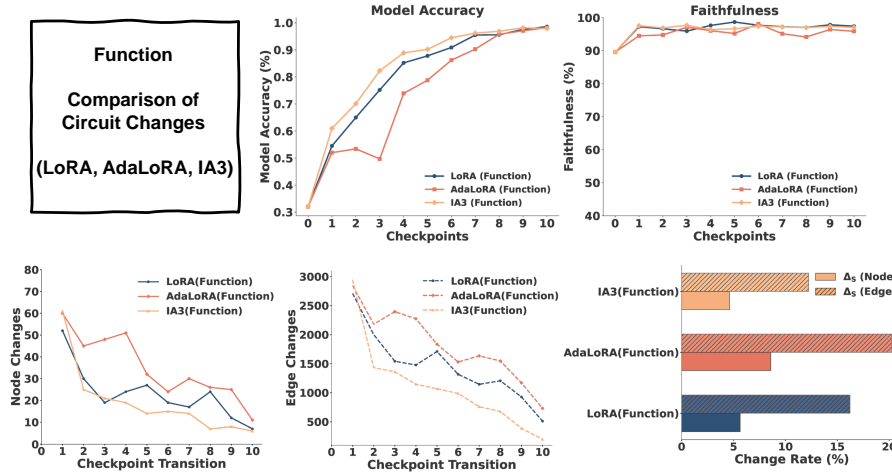

Figure 15: **Comparison of Function circuits during fine-tuning with LoRA, AdaLoRA, and IA3.** **Top:** Model accuracy and faithfulness across checkpoints. **Bottom Left:** Node and edge changes across checkpoint transitions. **Bottom Right:** Change rate of nodes and edges during fine-tuning.

checkpoints and the corresponding change rates. By examining these metrics, we can gain insights into how the internal circuits evolve under different model sizes and architectures.

Circuits in the addition/subtraction task converge across all models, with edge change rates consistently exceeding node change rates. Fine-tuning in each model creates new circuits through significant reconfiguration of connections among components.

Larger models exhibit higher node and edge change rates. As shown in Figure 17, the opt-6.7B model demonstrates the largest change rates, while the faithfulness of its discovered circuit remains stable throughout fine-tuning.
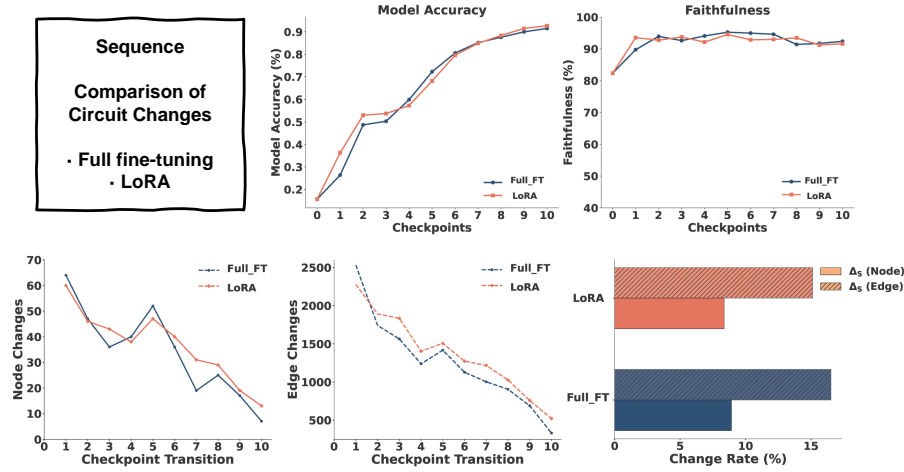
22

Figure 16: **Comparison of circuit changes during fine-tuning between Full Parameter Fine-Tuning (Full-FT) and LoRA. Top:** Model accuracy and faithfulness across checkpoints. **Bottom Left:** Node and edge changes across checkpoint transitions. **Bottom Right:** Change rate of nodes and edges during fine-tuning.
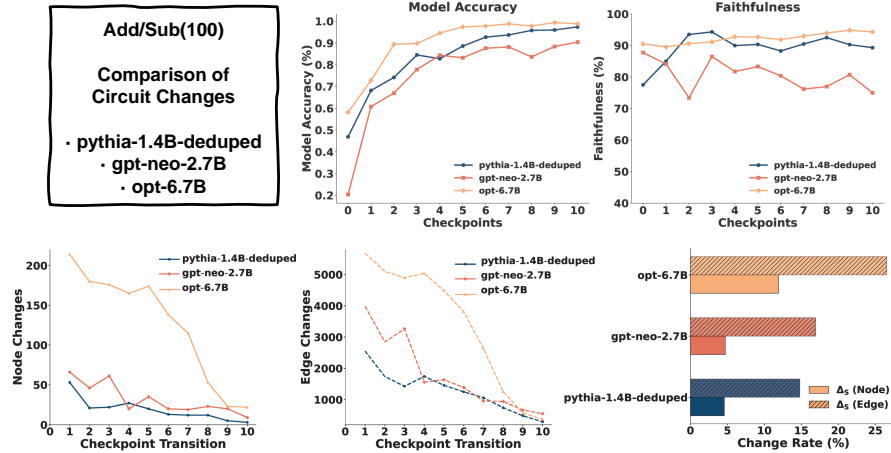

Figure 17: **Comparison of circuit fine-tuning changes between different LLMs (pythia-1.4B-deduped, gpt-neo-2.7B, opt-6.7B). Top:** Model accuracy and faithfulness across checkpoints. **Bottom Left:** Node and edge changes across checkpoint transitions. **Bottom Right:** Change rate of nodes and edges during fine-tuning.

Therefore, using different model architectures and sizes, we consistently observe the conclusions presented in Section 3.2 and Section 3.3: *Circuit Convergence During Fine-Tuning* and *Reorganization of Circuit Edges to Form a New Circuit.*

J CIRCUITLORA PERFORMANCE ON OTHER TASKS

In this appendix, we extend our investigation of `CircuitLoRA` to additional tasks beyond those discussed in the main text. These tasks include a variety of numerical operations, such as addition and subtraction with varying ranges, to further examine the performance and robustness of our circuit-aware fine-tuning approach. By testing `CircuitLoRA` on these additional benchmarks,

we aim to provide a more comprehensive evaluation, highlighting how incorporating circuit-based insights can yield consistent gains across a broader set of mathematical tasks.

Table 4: **Performance metrics for addition and subtraction across various configurations in different numerical ranges.** The control groups of `CircuitLoRA` ($r_o = 8$, $r_c = 32$) are LoRA ($r_o = 16$) and RandomLoRA ($r_o = 8$, $r_c = 32$), and the control groups of `CircuitLoRA` ($r_o = 32$, $r_c = 64$) are LoRA ($r_o = 32$) and RandomLoRA ($r_o = 32$, $r_c = 64$). Here, r_o and r_c represent the ranks used in `CircuitLoRA`, where r_c is the rank for *critical layer* modules, and r_o is the rank for *non-critical layer* modules. Model Accuracy is expressed as percentages.

Method	Parameter Ratio	Add/Sub(100)	Add/Sub(200)	Add/Sub(400)	Add/Sub(500)
Pre-trained	0%	46.90	24.90	12.20	9.90
Full FT	100%	96.80	90.50	75.30	63.60
LoRA ($r_o = 2$)	0.1111%	94.40	82.90	68.90	55.60
LoRA ($r_o = 8$)	0.4428%	95.40	86.40	73.10	64.30
LoRA ($r_o = 16$)	0.8816%	96.70	87.80	77.90	68.30
LoRA ($r_o = 32$)	1.7479%	97.40	90.30	78.20	69.70
CircuitLoRA ($r_o = 8$, $r_c = 32$)	0.7175%	**96.90**	**90.40**	**77.90**	**70.60**
RandomLoRA ($r_o = 8$, $r_c = 32$)	0.7175%	95.70	87.30	73.30	63.70
CircuitLoRA ($r_o = 32$, $r_c = 64$)	1.4248%	**97.90**	**91.00**	**78.20**	**73.00**
RandomLoRA ($r_o = 32$, $r_c = 64$)	1.4248%	97.00	89.60	77.70	64.20

In summary, the results presented in Table 4 demonstrate that `CircuitLoRA` maintains its advantage over both LoRA and RandomLoRA baselines across multiple configurations and numerical ranges. Even when the parameter ratio is constrained, `CircuitLoRA` effectively identifies and prioritizes *Critical Layers*, ensuring superior accuracy compared to methods that allocate ranks uniformly or randomly. These findings further validate the effectiveness of circuit-based analysis in enhancing fine-tuning efficiency and performance, reinforcing **Key Observation 3**: *Circuits can improve fine-tuning by achieving higher accuracy and parameter efficiency across various mathematical tasks.* In the addition and subtraction task, we can see that after using `CircuitLoRA` ($r_o = 8$, $r_c = 32$), we can achieve almost the same accuracy or even higher with half the training parameters of LoRA ($r_o = 32$).

K EXAMPLES OF COMPOSITIONAL TASK

Our compositional task involve two-step arithmetic operations, requiring reasoning across different mathematical operations. This task requires the model to perform addition and subtraction operations first, and then multiplication and division operations. The following examples demonstrate a diverse set of arithmetic problems designed for this purpose.

Example:

- ```
  Clean:  Calculate the result of the following arithmetic
  expression and provide only the final answer:  (43 - 7) * 21
  =
  ```

- ```
  Corrupted:  Calculate the result of the following arithmetic
  expression and provide only the final answer:  (43 - 7) * 88
  =
  ```

Example:

- ```
  Clean:  Calculate the result of the following arithmetic
  expression and provide only the final answer:  (82 - 43) /
  13 =
  ```

- ```
  Corrupted:  Calculate the result of the following arithmetic
  expression and provide only the final answer:  (82 - 43) / 3
  =
  ```

These tasks demonstrate each example in this task can be divided into two subtasks: addition and subtraction tasks and multiplication and division tasks. The purpose of this task is to see whether the

circuit in the combination task can be approximately replaced by the union of the circuits of the two subtasks. This provides ideas and experimental basis for exploring more complex combination tasks.